

# MBE Growth and Characteristics of Periodic Index Separate Confinement Heterostructure InGaAs Quantum-Well Lasers

M. HONG, M. C. WU, Y. K. CHEN, J. P. MANNAERTS, and M. A. CHIN

AT&T Bell Laboratories, Murray Hill, NJ 07974

We have used solid-source molecular beam epitaxy (MBE) to grow InGaAs quantum-well lasers emitting at 980nm in a novel configuration of periodic index separate confinement heterostructure (PINSCH). Periodic multilayers (GaAs/AlGaAs) are utilized as optical confinement layers to reduce the transverse beam divergence as well as to increase the maximum output power. The multilayers are grown by temperature modulation MBE without any shutter operation. The heterointerfaces in the multilayers are linearly graded such that the energy barrier heights are greatly decreased. This has led to a drastic reduction in the series resistance which is essential in the performance of high output power. The  $5\mu\text{m} \times 750\mu\text{m}$  device has far-field angles of  $10^\circ$  by  $20^\circ$ , a threshold current of 45 mA, an external differential quantum efficiency of 1.15 mW/mA (90%), and an output power of 620 mW, all measured at room temperature under CW operation. A record high fiber coupling efficiency of 51% has been achieved and more than 130 mW of power is coupled into a  $5\mu\text{m}$ -core single mode fiber.

**Key words:** Molecular beam epitaxy, PINSCH lasers, InGaAs quantum wells

## INTRODUCTION

High power semiconductor lasers emitting at 980 nm find applications in erbium doped fiber amplifiers (EDFA).<sup>1</sup> Lasers using a conventional graded-index separate confinement heterostructure (GRINSCH) have produced low threshold currents and high quantum efficiencies.<sup>2</sup> However, the tight optical confinement of the GRINSCH structure generates large beam divergence in the direction perpendicular to the junction plane ( $\sim 50^\circ$  for InGaAs/AlGaAs lasers<sup>1</sup>). This then gives a highly elliptical far-field pattern, and consequently, results in low coupling efficiency of the lasers into optical fibers. The beam divergence can be reduced by expanding the transverse mode size in the laser cavity. Previous approaches to achieve this goal include the use of large optical cavities<sup>3</sup> and vertically coupled active/passive waveguides.<sup>4,5</sup> More recently, we have proposed and demonstrated a novel quantum-well (QW) laser using a configuration of periodic index separate confinement heterostructure (PINSCH) to reduce the beam divergence.<sup>6</sup> The laser was grown by the solid-source molecular beam epitaxy (MBE) with ability to modulate the cell temperatures.<sup>7</sup> The transverse beam in the PINSCH laser is reduced to  $20^\circ$ , along with attainment of a high output power exceeding 620 mW.

In this paper, we first explain the concept of the PINSCH laser. Detailed growth parameters on temperature modulation MBE are given. A comparison between this new growth technique and conventional MBE approaches is discussed. Finally, we present processing and characteristics of this new laser.

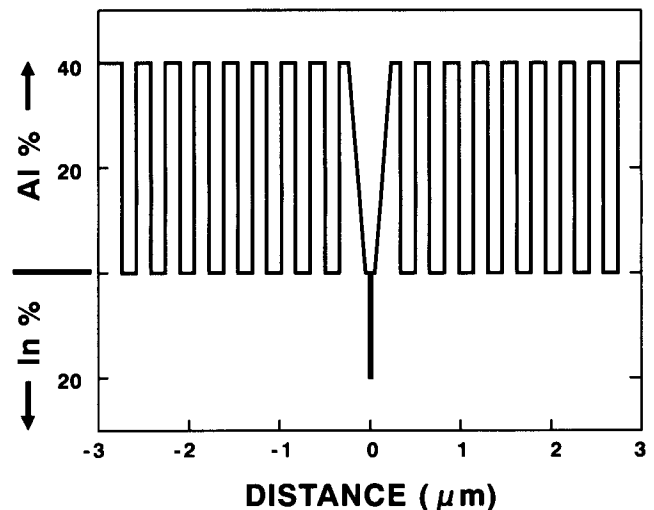


Fig. 1 — The layer composition of the PINSCH quantum well laser. Only a few pairs of AlGaAs/GaAs are needed for the PINSCH confining layers.

## DEVICE CONCEPT

Figure 1 is a schematic of the PINSCH laser which consists of three parts: an active region in the center and periodic-index (PIN) confinement layers on either side of the active region. The active region comprises three  $\text{In}_{0.2}\text{Ga}_{0.8}\text{As}$  quantum wells  $70\text{\AA}$  thick and four GaAs barriers  $200\text{\AA}$  thick. Each PIN confinement layer consists of eight pairs of  $\text{Al}_{0.4}\text{Ga}_{0.6}\text{As}/\text{GaAs}$  periodic multilayers.

The concept of the PINSCH laser has been explained elsewhere.<sup>6</sup> In brief, the principle of the single transverse modes operation is similar to that of the single longitudinal mode operation in a quarter-wave shifted distributed feedback ( $\lambda/4$ -DFB) laser widely used in optical communication systems.<sup>8,9</sup> In

the  $\lambda/4$ -DFB lasers the optical waves propagate perpendicular to the periodic media and the Bragg reflection condition applies to the longitudinal modes, while in the PINSCH lasers the optical waves propagate parallel to the periodic multilayers and the Bragg condition applies to the transverse modes.

The advantages of the PINSCH laser are that the transverse optical mode profile can be independently synthesized and expanded, while the electrical carrier confinement is as good as that of the GRINSCH structure. Synthesis of the transverse mode size is carried out by adjusting the layer thicknesses of the periodic media. Moreover, all the high-order transverse modes are totally suppressed in the PINSCH structure. The suppression of high-order spatial modes is very important for applications which require diffraction-limited beam profile and high efficiency in light collection. The expansion of the transverse mode size reduces the optical power density in the cavity. Therefore, a higher power can be obtained before it is limited by the catastrophic optical damage (COD). In fact, a thermally limited output power exceeding 620 mW is obtained from a 5  $\mu\text{m}$ -wide AR/HR-coated ridge-waveguide PINSCH laser as will be discussed later in the paper.

In actual implementation of the PINSCH lasers, only a finite number of PIN layers are needed because the optical field decays quickly within a couple of periods. Eight pairs of  $\text{Al}_{0.4}\text{Ga}_{0.6}\text{As}$  and GaAs are used in our experiments here. The thickness of the  $\text{Al}_{0.4}\text{Ga}_{0.6}\text{As}$  and GaAs layers are designed to be the same of 0.16  $\mu\text{m}$ . In addition, the last  $\text{Al}_{0.4}\text{Ga}_{0.6}\text{As}$  layers adjacent to the active region are combined with the GaAs layers in the core region so that the Al concentration is linearly graded toward the quantum wells to enhance the electrical carrier confinement. The active region of the PINSCH laser is similar to that of the GRINSCH lasers, in which good carrier confinement and low threshold current operation have been demonstrated.

## MBE GROWTH

A precise control (within 5–10%) of the layer thickness and composition is required for the PINSCH structure. The accurate growth rates of GaAs, AlAs, and AlGaAs depend on careful calibration using reflection high energy electron diffraction (RHEED) oscillations, flux gauge measurement near the substrate, optical reflectivity measurements, and high resolution x-ray diffraction. The results from the first two experiments lead to the starting point in determining the growth parameters such as cell temperatures of Al and Ga, and time intervals for the PIN layers as well as the active region. The fine tuning in the growth parameters relies on the latter two measurements which were carried out on samples with a periodic structure consisting of, for example, GaAs and AlAs, or AlGaAs with different Al mole fractions. The detailed experimental procedures using the optical re-

flectivity and x-ray diffraction in determining the layer composition and thickness are given elsewhere.<sup>10</sup>

For growing periodic GaAs/AlGaAs multilayers with sharp interfaces, cell temperatures of Ga and Al remain constant to give a desirable growth rate, and the fluxes of Ga and Al are controlled only by the shutters just above the cells through an open/close operation. For growing the PIN (GaAs/ $\text{Al}_{0.4}\text{Ga}_{0.6}\text{As}$ ) layers here, we have used a completely different approach. We have modulated the cell temperatures of Al and Ga without any shutter operation. During the growth of the multilayers, the shutters for Ga and Al are kept open. In other words, the fluxes of Ga and Al are controlled only by the cell temperatures. For example, in growing the GaAs layer, the Al cell temperature is kept low such that no flux comes out of the cell. In growing the interfaces, the cell temperatures of Al and Ga are simultaneously varied to give a linearly compositional profile. This new technique of temperature modulation MBE has also been successfully applied to grow vertical cavity surface emitting lasers. Note that more stringent growth parameters are required in the surface emitting lasers (to within 3%).

Given the same cell temperatures of Si and Be, the *n*- or *p*-type carrier concentration of AlGaAs is a function of Al mole fraction. In the Si case, decrease in the carrier concentration was observed around the direct-indirect band crossover point.<sup>11</sup> In the Be case, the carrier concentration is roughly a linear function of Al mole fraction from GaAs to AlAs.<sup>10</sup> Therefore, the cell temperatures of Si and Be have also to be modulated in order to achieve the designed doping profiles as shown in Fig. 2. Note that using our new temperature modulation MBE, the growth rates for GaAs,  $\text{Al}_{0.4}\text{Ga}_{0.6}\text{As}$ , and the graded area are kept constant. This makes it easy in producing desirable doping profiles and in keeping minimal As overpressure necessary for good growth of GaAs and AlGaAs. The cell temperatures and their modulations measured by the thermal couples are shown in Fig. 2 for a typical growth of the PINSCH laser. The thickness of the linearly graded hetero-interfaces is  $\sim 500\text{\AA}$ .

In a theoretical calculation using the Fermi-Dirac statistics and a self-consistent method to solve the Poisson equation, the valence and conduction band diagrams of the GaAs/ $\text{Al}_{0.4}\text{Ga}_{0.6}\text{As}$  with sharp interfaces and linearly graded interfaces have been depicted.<sup>12</sup> It is found that the large energy barrier with a spike at the interface of GaAs and  $\text{Al}_{0.4}\text{Ga}_{0.6}\text{As}$  caused by the presence of sharp interfaces has been greatly reduced in the case of linearly graded interfaces for the same level of *p*- or *n*-doping. As a consequence, low resistance has been achieved without employing high doping at the hetero-interfaces, which would increase the cavity loss due to free-carrier absorption. The doping levels are  $0.2 - 1.0 \times 10^{18}\text{cm}^{-3}$  for the *n*-type and  $1.0 \times 10^{18}\text{cm}^{-3}$  for the *p*-type. The active region and the adjacent 500 $\text{\AA}$  in the confinement layers are undoped. The doping levels are similar to those of conventional

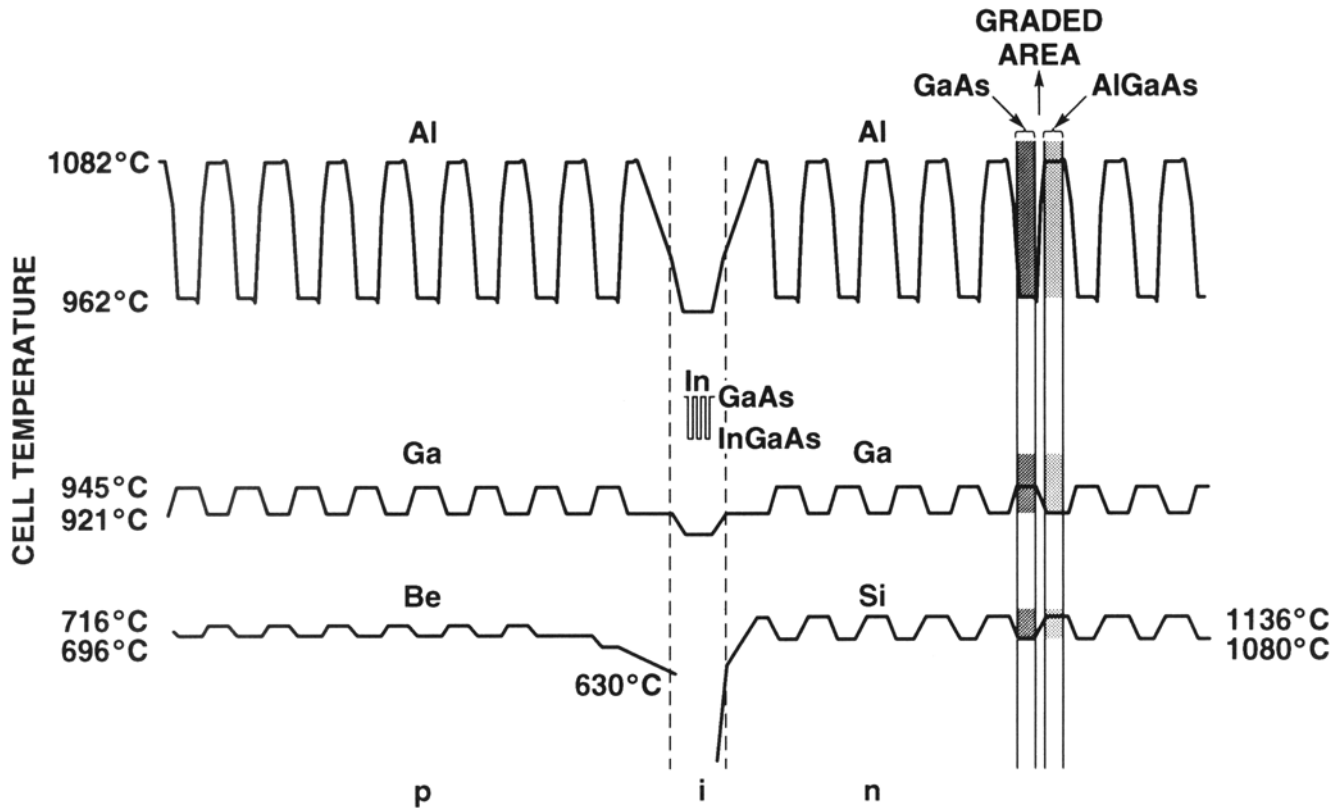


Fig. 2 — Cell temperatures of Ga, Al, Si, and Be during the shutterless growth of a typical PINSCH laser. The central area including the active region and  $\sim 500\text{\AA}$  of the confining layers on each side of the active region.

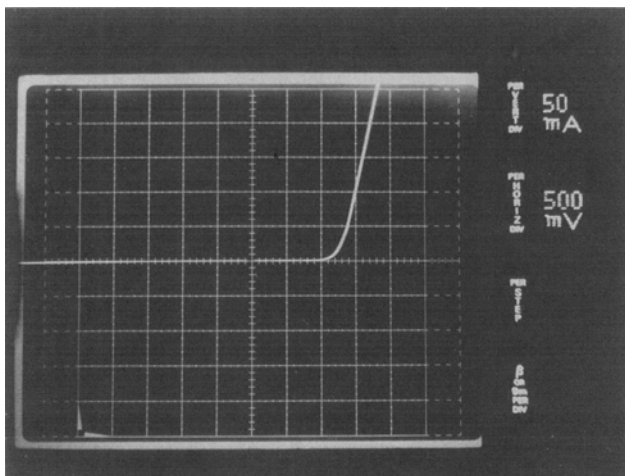


Fig. 3 — I-V characteristics of self-aligned PINSCH ridge-waveguide laser. This laser is  $4\ \mu\text{m}$  wide and  $750\ \mu\text{m}$  long.

GRINSCH lasers. A series resistance as small as  $2\ \Omega$  is achieved for a  $4\ \mu\text{m} \times 750\ \mu\text{m}$  PINSCH laser as shown in Fig. 3 of an I-V curve. This value is similar to those obtained in GRINSCH lasers. The graded interfaces by the temperature modulation MBE certainly make low resistance despite the presence of 32 heterojunctions (16 pairs of GaAs/ $\text{Al}_{0.4}\text{Ga}_{0.6}\text{As}$  with 2 interfaces in each pair) in the PINSCH laser.

The substrate temperature during growth is kept

constant at  $600^\circ\text{C}$  for precise control of the layer thickness and composition even for the growth of  $\text{Al}_{0.4}\text{Ga}_{0.6}\text{As}$ . However, for the growth of the active region including  $\text{In}_{0.2}\text{Ga}_{0.8}\text{As}$ , the substrate temperature was lowered to  $550\text{--}560^\circ\text{C}$ . This growth condition has consistently given the PINSCH structure lasing at  $980\ \text{nm}$ .

### PROCESSING AND PERFORMANCE OF PINSCH LASER

Ridge-waveguide PINSCH lasers are fabricated using a previously reported self-aligned process.<sup>13</sup> The cross-sectional secondary electron micrograph (SEM) of the device is shown in Fig. 4. A  $5\ \mu\text{m}$ -wide ridge waveguide is formed by wet chemical etching and planarized by polyimide. The thickness of the remaining cladding layer above the active quantum wells is  $0.45\ \mu\text{m}$ , about one pair of AlGaAs/GaAs PIN confinement layers. Note that because of the expansion of the transverse mode size, the required residual cladding layer thickness for single lateral mode operation is much larger than that required in the GRINSCH lasers. Though higher threshold current densities than that of the GRINSCH lasers are expected because of the lower optical confinement factors, a value of  $500\ \text{A}/\text{cm}^2$  is achieved from the broad area laser with a typical size of  $127\ \mu\text{m} \times 254\ \mu\text{m}$ . Further reduction of the threshold current densities is likely with optimized structures and

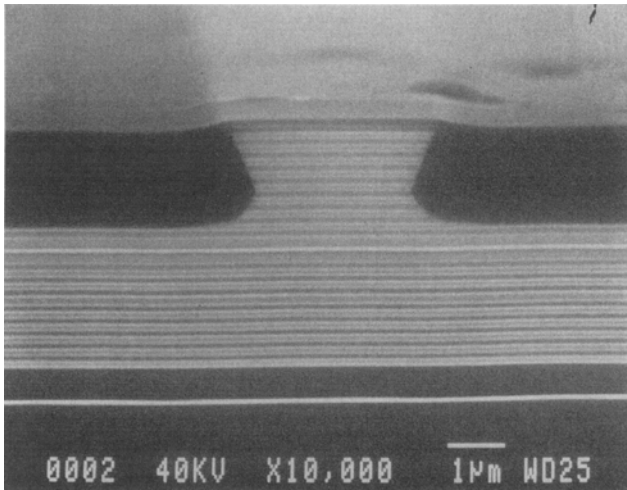


Fig. 4 — The cross-sectional SEM micrograph of the self-aligned PINSCH ridge-waveguide laser.

growth conditions. The room temperature continuous wave (CW) light-versus-current (L-I) curve of a self-aligned ridge-waveguide PINSCH laser 750  $\mu\text{m}$  long is shown in Fig. 5. The reflectivities of the front and back facets are about 10% and 90%, respectively, after coatings. A threshold current of 45 mA and an external differential quantum efficiency of 1.15 mW/mA (90%) are achieved. Note that the threshold current of 45 mA corresponds to a threshold current density of 1.2  $\text{kA}/\text{cm}^2$ . The higher threshold in the device is caused by the current spreading in the ridge waveguide structure. The CW

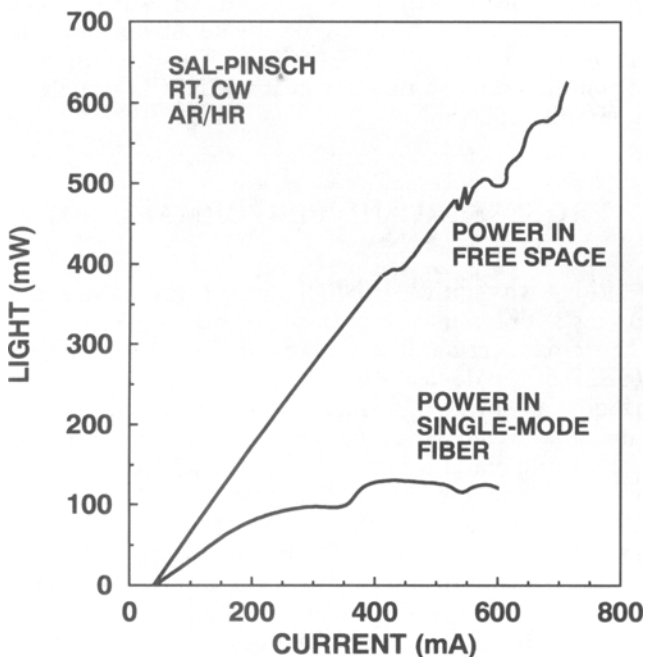


Fig. 5 — The room temperature CW L-I curves of a 5  $\mu\text{m} \times 750 \mu\text{m}$  PINSCH laser showing output power in free space and coupled into a single mode fiber with 5  $\mu\text{m}$  core diameter.<sup>6</sup> The maximum output powers in free space and in the fiber are 620 and 130 mW, respectively. The output power of 620 mW is thermally limited.

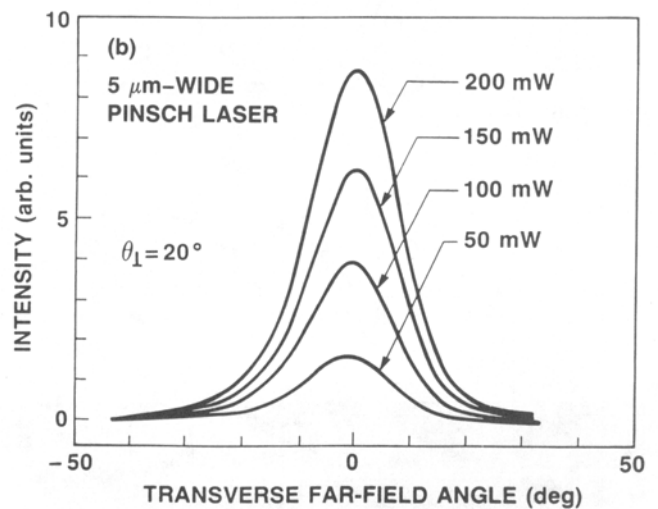
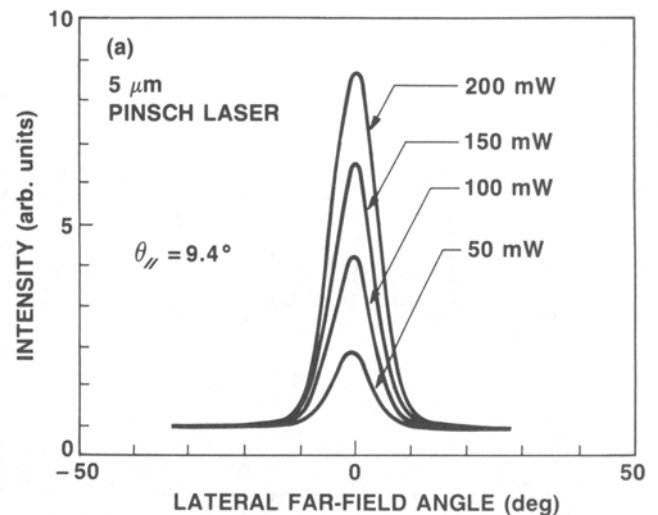


Fig. 6 — The lateral (a) and transverse (b) far-field patterns of the PINSCH laser at 50 mW, 100 mW, 150 mW, and 200 mW. The FWHM angles are  $\theta_{\parallel} = 9.4^{\circ}$  and  $\theta_{\perp} = 20^{\circ}$ , respectively.<sup>6</sup>

output power into free space exceeds 620 mW at a pump current of 700 mA, which is not yet limited by COD. Normalizing the power with the width of the laser, the maximum output power is 120  $\text{mW}/\mu\text{m}$ , the highest value ever reported for ridge-waveguide strained-layer InGaAs quantum well lasers.

The transverse mode is guided by the PINSCH structure and the lateral mode is index-guided by the ridge waveguide. The lateral and transverse far-field patterns of the PINSCH laser are shown in Fig. 6(a) and (b), respectively. Single transverse-mode operation with full-width-at-half-maximum (FWHM) far-field angles of  $\theta_{\parallel} = 20^{\circ}$  is observed for all output power levels. On the other hand, single lateral mode operation with  $\theta_{\perp} = 9.4^{\circ}$  is obtained only up to 150 mW. The strong nonlinearities which are present in the light vs current plot (Fig. 5) are due to the appearance of high-order lateral modes. The exact current and power level varies from laser to laser. With a better control of the ridge width, the high-order lateral modes can be suppressed. The  $\theta_{\perp}/\theta_{\parallel}$  ratio is 2.1, about two to three times better than that

of the InGaAs/AlGaAs GRINSCH lasers. The more symmetric beam profile greatly increases the optical coupling efficiency into optical fibers. A coupling efficiency of 51% is obtained and more than 130 mW of power is coupled into a 5  $\mu\text{m}$ -core single mode fiber. In addition to the high coupling efficiency, the low beam divergence also allows the use of lenses with a lower numerical aperture. Thus the alignment tolerance is greatly relaxed.

## CONCLUSION

We have grown, fabricated, and demonstrated InGaAs quantum well lasers emitting at 980 nm in periodic index separate confinement heterostructure (PINSCH). Our solid-source MBE with an ability of modulating cell temperatures has been fine tuned to grow the structure. In particular, the periodic-index (PIN) multilayers were grown without any shutter operation. The linearly graded interface between GaAs and  $\text{Al}_{0.4}\text{Ga}_{0.6}\text{As}$  resulted from the simultaneous modulation of Al and Ga cell temperatures and the shutterless operation has drastically reduced the energy barrier heights at the heterointerface. This, as a consequence, drastically reduces the series resistance without a high doping. Therefore, a high output power performance under a room temperature CW operation has been realized.

The PINSCH structure expands the fundamental transverse mode size while totally suppressing the high-order modes and efficiently confining the injected electrical carriers. A transverse beam divergence of  $20^\circ$  is obtained with a moderate increase of

the threshold current density ( $500 \text{ A/cm}^2$ ). With a self-aligned ridge-waveguide structure, the 5  $\mu\text{m}$ -wide and 750  $\mu\text{m}$ -long PINSCH laser emitting at 980 nm has a CW threshold current of 45 mA, an external quantum efficiency of 1.15 mW/mA (90%), and a CW output power exceeding 620 mW. Stable far-field patterns of  $10^\circ$  by  $20^\circ$  and a record high coupling efficiency of 51% into single mode fiber are achieved. More than 130 mW of power is coupled into the fiber, the highest value ever reported at the wavelength of 980 nm.

## REFERENCES

1. S. Uehara, M. Okayasu, T. Takeshita, O. Kogure, M. Yamada, M. Shimizu and M. Horiguchi, *Optoelectron.* **5**, 71 (1990).
2. W. T. Tsang, *Appl. Phys. Lett.* **40**, 217 (1982).
3. H. F. Lockwood, H. Kressel, H. S. Sommers and F. Z. Harylo, *Appl. Phys. Lett.* **17**, 499 (1970).
4. R. G. Waters, M. A. Emanuel and R. J. Dalby, *J. Appl. Phys.* **66**, 961 (1989).
5. Y. C. Chen, R. G. Waters and R. J. Dalby, *Electron. Lett.* **26**, 1348 (1990).
6. M. C. Wu, Y. K. Chen, M. Hong, J. P. Mannaerts, M. A. Chin and A. M. Sergent, *Appl. Phys. Lett.* **59**, 1046 (1991).
7. M. Hong, J. P. Mannaerts, J. M. Hong, R. J. Fischer, K. Tai, J. Kwo, J. M. Vandenberg, Y. H. Wang and J. Gamelin, *J. Cryst. Growth* **111**, 1071 (1991).
8. H. Kogelnik and C. V. Shank, *J. Appl. Phys.* **43**, 2328 (1972).
9. S. Wang, *IEEE J. Quantum Electron.* *QE-10*, 413 (1973).
10. M. Hong, J. P. Mannaerts, J. M. Vandenberg, J. R. Kwo and J. Gamelin, unpublished results.
11. T. Ishibashi, S. Tarucha and H. Okamoto, *Jpn. J. Appl. Phys.* **21**, L476 (1982).
12. J. M. Hong and J. Gamelin, private communication.
13. Y. K. Chen, M. C. Wu, W. S. Hobson, S. J. Pearton, A. M. Sergent and M. A. Chin, to be published in *Photon. Tech. Lett.* (1991).